Journal of Applied Polymer Science

Epoxide-terminated hyperbranched polyether sulphone as triple enhancement modifier for DGEBA

Xuepei Miao,[1,2] Yan Meng,[2] Xiaoyu Li[1]

[1]State Key Laboratory of Organic-Inorganic Composites, Beijing University of Chemical Technology, Beijing 100029, People's Republic of China

[2]Key Laboratory of Carbon Fiber and Functional Polymers, Ministry of Education, College of Materials Science and Engineering, Beijing University of Chemical Technology, Beijing 100029, People's Republic of China

Correspondence to: Y. Meng (E-mail: mengyan@mail.buct.edu.cn) and X. Li (E-mail: lixy@mail.buct.edu.cn)

ABSTRACT: Epoxide-terminated hyperbranched polyether sulphones (EHBPESs) with different backbone structures were synthesized and used as tougheners for diglycidyl ether of bisphenol-A (DGEBA) curing system, which result in nonphase-separated cured networks. Effects of backbone structure (at comparable degree of polymerization) and loading contents on the mechanical and thermal properties of cured hybrids were investigated. The hybrid containing EHBPES3, which has the most flexible backbone, shows the best mechanical performance and highest glass transition temperature (T_g). Compared with unmodified system, the impact strength, tensile strength, elongation at break of the hybrid containing 5% EHBPES3 increased by 69.8%, 9.4%, and 60.2%, respectively. The balanced improvements were attributed to the increased crosslink density and fractional free volume as well as the unique inhomogeneous network structure because of incorporation of hyperbranched modifiers with proper structure and loading contents.
 J. Appl. Polym. Sci. **2015**, *132*, 41910.

KEYWORDS: dendrimers; hyperbranched polymers and macrocycles; mechanical properties; structure-property relations; thermal properties; thermosets

Received 20 October 2014; accepted 24 December 2014

DOI: 10.1002/app.41910

INTRODUCTION

Epoxy resins are versatile thermosetting polymers and have been used in many applications due to their low cure shrinkage, good solvent, and chemical resistance, excellent adhesion, and mechanical properties.[1,2] However, in some advanced applications, their applicability is restrained by their inherent brittleness and low toughness.[3] Therefore, epoxy toughening has long been a focus in both academic and industrial filed. Epoxy resins can be toughened by adding different types of tougheners, such as nanoinorganic particles,[4] thermoplastic resin,[5] rubber particles,[6] and core-shell polymer particles.[7] When liquid rubber and core-shell particles are blended with epoxy, improved toughness are often achieved at the expense of glass transition temperature (T_g) and tensile strength.[6,7] Although nanoinorganic particles and thermoplastic resin can toughen epoxy without decreasing T_g, high mixing viscosity and surface treatments could compromise processability.[4,5] In addition, effects of toughening depend heavily on the final phase-separated morphology, which is not always easy to control, especially in fiber-reinforced composites. So far, the search for new tougheners that can form nonphase-separated network without compromising strength and T_g is still challenging.[8–12] Recently, hyperbranched polymers (HBPs) have showed great potential as a new type of modifiers, which can toughen epoxy without compromising T_g and other mechanical properties.[13–17] The balanced improvements are often attributed to the special structures of hyperbranched tougheners, e.g., highly compacted semispherical shape, large numbers of terminal groups, and internal molecule-scale cavities.[18–22] HBPs can be synthesized using simple one-pot procedure, making them much cheaper and easier to produce than dendrimers.[23,24] Epoxide- or hydroxyl-terminated HBP can be used as reactive tougheners for epoxy. Among them, hyperbranched polyesters (Boltorn™) had been extensively studied.[25–27] However, similar to rubber toughening, epoxies toughened by Boltorn™ modifiers also form phase-separated morphology and show decreases in tensile strength and T_g. Recently, Zhang *et al.* reported a series of hyperbranched polyester with aromatic ester backbones, which can toughen epoxy without forming phase separation; however, improved toughness and tensile strength are accompanied by big reduction in T_g.[22,28,29] Jin and Park reported a hyperbranched polyimide, which can toughen diglycidyl ether of bisphenol-A/diaminodiphenylmethane (DGEBA/DDM) system

without lowering T_g and forming phase-separated morphology; however, those modifiers are very costly.[30] Recently, HBPs with aromatic polyether backbone emerge as a new kind of promising low-cost tougheners, which have stiffer backbone and is chemically more stable than hyperbranched polyesters.[18–20] To the best of our knowledge, the synthesis of epoxy-terminated hyperbranched polyether sulphone and its application as nonphase-separated toughener have not been reported.

In this study, a series of epoxide-terminated hyperbranched polyether sulfones (EHBPESs), whose skeleton can be systematically tuned by changing the structure of B_3 monomers, were synthesized using one-pot $A_2 + B_3$ polycondensation reaction. Effects of toughening on backbone structure and loading contents were systematically explored by blending them into DGEBA/triethylene tetramine (TETA) curing system. Explanations for the dependence of mechanical properties on backbone structure and loading contents are also offered.

EXPERIMENTAL

Materials

Triethylenetetramine (TETA), tetrabutyl ammonium bromide (TBAB), and epichlorohydrin (ECH) were purchased from Tianjin Fu-Guang reagent Co. 4-Fluorophenyl sulfone (98%) was obtained from Zhongsheng Huateng Reagent. Trimethylolpropane (TMP) and *m*-trihydroxybenzene was purchased from Energy Chemistry (China). Diglycidyl ether of bisphenol A (DGEBA) was purchased from Yueyang Resin Factory, China (EEW = 190.04 g/equiv). Acetone-d_6, (dimethyl sulfoxide)-d_6, and $CDCl_3$ were purchased from Beijing InnoChem Science & Technology. Other reagents were purchased from Beijing reagent. 1-methyl-2-pyrrolidinone (NMP) and dimethyl sulfoxide (DMSO) were dried thoroughly before use. Triphenol methane was prepared by the reported approach.[18]

Synthesis of Hyperbranched Polyether Sulphone (HBPES)

HBPES1 was synthesized using one-pot $A_2 + B_3$ approach. Triphenol methane 35.04 g (0.12 mol), 22.88 g (0.09 mol) 4-Fluorophenyl sulfone, 49.68 g (0.36 mol) K_2CO_3, 583 ml NMP, and 145.75 ml toluene were charged into a three-necked flask equipped with a Dean-Stark trap, a condenser, and a nitrogen inlet. The flask was heated at 140°C for 60 min. The azeotrope of toluene and water was removed from the Dean-Stark trap. The flask was subsequently heated to 180°C for 5 h. After cooling to room temperature, the mixture was poured into 2000 ml acetic acid solution (0.1*M*). The precipitate was collected and reprecipitated from THF into ethanol. The resultant mixture was collected and dried under vacuum at 90°C to give a deep brick-red solid product with a yield of 73%. ^{1}H NMR (600 MHz, actone-d_6, δ): 5.46–5.63 (*m*, Ph_3CH—), 6.76–7.32 (*m*, C_6H_5O—), 7.90 (br, $SO_2C_6H_4O$—). IR (KBr): υ = 3410 (s), 2913 (m), 1660 (s), 1581 (m), 1487 (w), 1242 (m), 1147 (w), 1013 (m), 867 (w), 715 (w) cm^{-1}.

Following similar procedures as described above, HBPES2 and HBPES3 were prepared by reacting 4-fluorophenyl sulfone with m-trihydroxybenzene and TMP, respectively. Typical NMR and IR characterization results of HBPES2 and HBPES3 are given below. HBPES2: ^{1}H NMR (600 MHz, acetone-d_6, δ): 6.30-6.68 (*m*, $C_6H_3O_3$—), 6.96–7.30 (*m*, $C_6H_4O_3$—), 7.60–7.89 (*m*, $SO_2C_6H_4O$—). IR (KBr): υ = 3408 (s), 2913 (s), 1660 (m), 1593 (s), 1497 (m), 1414 (m), 1291 (s), 1150 (m), 1013 (m), 997 (w), 776 (w) cm^{-1}. HBPES3: ^{1}H NMR (600 MHz, acetone-d_6, δ): 0.91 (br, CH_3—), 1.40–1.71 (*m*, —$C(CH_2)_3$), 3.60–4.23 (*m*, —OCH_2C—), 6.96–7.80 (*m*, C_6H_4O—). IR (KBr) υ = 3514 (s), 2891–2937 (m), 1660 (s), 1593 (m), 1497 (m), 1409 (s), 1294 (m), 1149 (m), 1013 (m), 832 (w), 776 (w) cm^{-1}.

Synthesis of Epoxide-Terminated Hyperbranched Polyether Sulphone

Procedures for synthesizing three types of EHBPES are described one by one below. The detailed procedure for synthesizing EHBPES1 is as follows: 30.0 g HBPES1 and 5.7 g TBAB (the catalyst) were dissolved in 336 g of ECH. The mixture was heated to 110°C for 3 h under a dry nitrogen atmosphere. The resultant mixture was cooled to 50°C. 5.0 g of NaOH and 11.6 g H_2O were added dropwise into the mixture within 3 h using a peristaltic pump. The resultant mixture was kept at 50°C for another 2 h. After cooling to room temperature, the mixture was washed with hot water (>70°C) three times to remove residual salts. The resultant mixtures were dried with Mg_2SO_4 and then precipitated into ethanol. The precipitate was washed with ethanol and dried under vacuum at 90°C. The obtained EHBPES1 is a brick-red solid, and the yield is 70%. ^{1}H NMR (600 MHz, (DMSO)-d_6, δ): 2.55–2.71 (*m*, —CH_2—O—), 2.74–2.83 (*m*, —CH_2—O—), 3.20–3.33 (*m*, —CH—O—), 3.69–4.43 (*m*, —CH_2—O—), 5.29–5.63 (*m*, Ph_3CH—), 6.70–7.2 (*m*, C_6H_4O—), 7.76–7.90 (*m*, $SO_2C_6H_4O$—). IR (KBr) υ = 3514 (s), 2913 (m), 1660 (m), 1581 (s), 1487 (s), 1242 (m), 1147 (m), 1013 (m), 912 (m), 867 (w), 715 (w) cm^{-1}.

The procedure for preparing EHBPES2 is similar to that of EHBPES1. Thus only characterization results of EHBPES2 are given: ^{1}H NMR (600 MHz, (DMSO)-d_6, δ): 2.53–2.69 (*m*, —CH_2—O—), 2.70–2.85 (*m*, —CH_2—O—), 3.11–3.44 (*m*, —CH—O—), 3.69–4.43 (*m*, —CH_2—O—), 6.32–6.90 (*m*, $C_6H_3O_3$—), 6.90–7.30 (*m*, $C_6H_4O_3$—), 7.80–8.00 (*m*, $SO_2C_6H_4O$—); IR (KBr) υ = 3408 (s), 2913 (s), 1660 (m), 1593 (m), 1497 (m), 1414 (s), 1291 (m), 1150 (m), 1013 (m), 997 (m), 912 (m), 776 (w) cm^{-1}.

The procedure for preparing EHBPES3 is as follows. 30.0 g HBPES3 and 8.0 g KOH (the catalyst) were dissolved in 50 ml DMSO. The mixture was added into a three-necked flask equipped with mechanical stirring. After stirring at 23°C for 1 h, 336.0 g of ECH was added dropwise into the mixture using a peristaltic pump, and the resultant mixture was kept at 23°C for 15 h. The mixture was washed with hot water (>70°C) three times to remove residual salts. The resultant mixtures were dried with Mg_2SO_4 and then precipitated into ethanol. The precipitate was washed with ethanol and dried under vacuum at 80°C. The obtained EHBPES3 is an off-white solid with a yield of 72%. ^{1}H NMR (600 MHz, $CDCl_3$, δ): 0.86 (br, CH_3—), 1.25–1.81 (*m*, —$C(CH_2)_3$), 2.49–2.56 (*m*, —CH_2—O—), 2.66–2.74 (*m*, —CH_2—O—), 3.04–3.11 (*m*, —CH—O—), 3.20–4.05 (*m*, —OCH_2C—), 6.90–7.80 (*m*, C_6H_4O—). IR (KBr) υ = 3514 (s), 2891–2937 (s), 1660 (s), 1593 (m), 1497 (m), 1409 (m), 1294 (m), 1149 (s), 1013 (m), 912 (m), 832 (w), 776 (w) cm^{-1}.

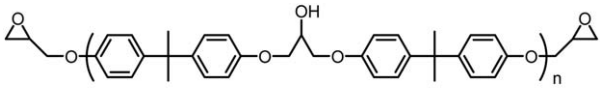

Diglycidyl ether of bisphenol A (DGEBA)

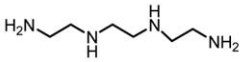

Triethylenetetramine (TETA)

Figure 1. Chemical structures of DGEBA and TETA.

Preparation of DGEBA/EHBPES Hybrids and Curing

The hybrid systems containing predetermined amounts (i.e., 3%, 5%, 10%, and 15% by total weights of epoxy) of EHBPES and DGEBA were prepared by mechanical mixing at 25°C. Stoichiometric amounts of TETA, the curing agent, were added in the mixture under continuously stirring at 25°C. The mixture were degassed and cured in silicone rubber molds to obtain cured samples in desirable shapes. The cure schedule followed a three-step procedure: cure at room temperature for 12 h, 100°C for 2 h, and 190°C for 2 h. After curing, cured samples were cool naturally to room temperature. Chemical structures of DGEBA and TETA are shown in Figure 1.

Characterization

^{1}H NMR spectra were collected using a Bruker AV-600 spectrometer (600 MHz). Acetone-d_6, (DMSO)-d_6, and $CDCl_3$ were the solvents used in NMR measurements. Number-average molecular weights (M_n) and the polydispersity index (PDI) of EHBPES samples were determined using a Waters 515-2410 gel permeation chromatography (GPC) system. The infrared spectra were recorded on a Bruker Tensor 37 spectrometer. The epoxy equivalent weights (EEW) were determined by titration using the HCl-acetone method.[31] Calorimetric data were determined by a DSC1 differential scanning calorimetry (Mettler-Toledo) at a heating rate of 10 K/min under nitrogen. Thermal stability in nitrogen was obtained using a Perkin-Elmer Pyris1 thermo gravimetric analyzer (TGA) from 30 to 800°C at a heating rate of 10 K/min. The dynamic mechanical properties at 1 Hz were measured using a TA Q800 dynamic mechanical analyzer (DMA) in the single cantilever mode. Measurements were performed on heating runs from 50 to 220°C at 5°C/min. Linear coefficients of thermal expansion (LCTE, denoted by α_l) were measured using a Mettler-Toledo TMA/SDTA841e Thermal Mechanical Analyzer during cooling runs from 190 to 40°C at 2 K/min. The tensile properties were characterized by an Instron 1185 test machine according to ISO 527:1993. Unnotched impact strength tests were performed on a Ceast Resil impact tester according to ISO 179:1982. For each composition, at least ten samples were measured. After impact and tensile tests, fracture surfaces were scanned by a JEOL JSM-6700 Scanning Electron Microscopy (SEM) at 5 kV.

RESULTS AND DISCUSSION

Characterization of Synthesized Polymers

The characterization results of three EHBPESs are shown in Table I. All three types of EHBPES samples have similar M_n, i.e., ~2000 g/mol, indicating that they have similar average degree of polymerization. We note that the M_n of EHBPESs determined from GPC could be smaller than the actual values. However, recent studies[32,33] clearly showed that the M_n of hyperbranched molecules obtained from GPC method is actually very close to true values if the M_n is less than 10,000 g/mol, and notable deviation between GPC determined M_n and true M_n value is only observed when M_n is above 10,000 g/mol. As a result, considering the small M_n (<3000 g/mol) of our EHBPES samples, M_n determined from GPC should not deviate obviously from actual values. Theoretical EEW (EEW_{the}) and experimental EEW (EEW_{exp}) were also supplied in Table I. It is clear that the difference between EEW_{exp} and EEW_{the} is indeed very small. In addition, EHBPES3, which has more flexible backbone, shows the lowest EEW. When 4-fluorophenyl sulfone is reacted with triphenol methane, *m*-trihydroxybenzene, and TMP, the obtained HBPES are labeled as HBPES1, HBPES2, and HBPES3, respectively. When ECH is reacted with HBPES1, HBPES2, and HBPES3, the obtained EHBPES are labeled as EHBPES1, EHBPES2, and EHBPES3, respectively. The idealized structures of EHBPESs are shown in Figure 2, and the structures of EHBPESs were confirmed by IR and NMR measurements.

The degree of branching (DB) of hyperbranched polymer can be calculated according to the following equation,[34] $DB = (D + T)/(D + T + L)$, where the D, T, and L are the numbers of dendritic, terminal, and linearly units in the hyperbranched polymer, which can be obtained using NMR spectroscopy. DB of EHBPES samples were summarized in Table I. Clearly, these three EHBPESs show very similar DB values.

DSC Characterization

DSC curves of neat DGEBA system and hybrids at different loadings of EHBPES3 are shown in Figure 3. In Figure 3(a), the onset cure temperature of hybrids decreases with loadings, indicating that addition of EHBPES3 can increase the reactivity of epoxide group. In Figure 3(b), the onset cure temperature of EHBPES3 is lower than those of EHBPES2 and EHBPES1, confirming that EHBPES3 has higher reactivity. For hybrid with different loading of EHBPES3, heats of reaction are shown in Table II. At low loadings (3% and 5%), the heat of reaction per mole of epoxide groups (ΔH_{tot}) increases with EHBPES3 loading. Because of the higher functionality of EHBPES, addition of

Table I. Physical Properties of EHBPESs

Sample	M_n (g mol^{-1})	PDI	EEW_{exp}	EEW_{the}	DB	T_g (°C)	T_{d5} (°C)	Char yield at 600°C (%)
EHBPES1	2800	1.47	400.0	384.6	0.56	141.94	391.72	53
EHBPES2	1700	1.66	370.4	324.5	0.59	184.72	422.35	51
EHBPES3	2000	2.10	312.5	289.9	0.58	62.36	397.14	20

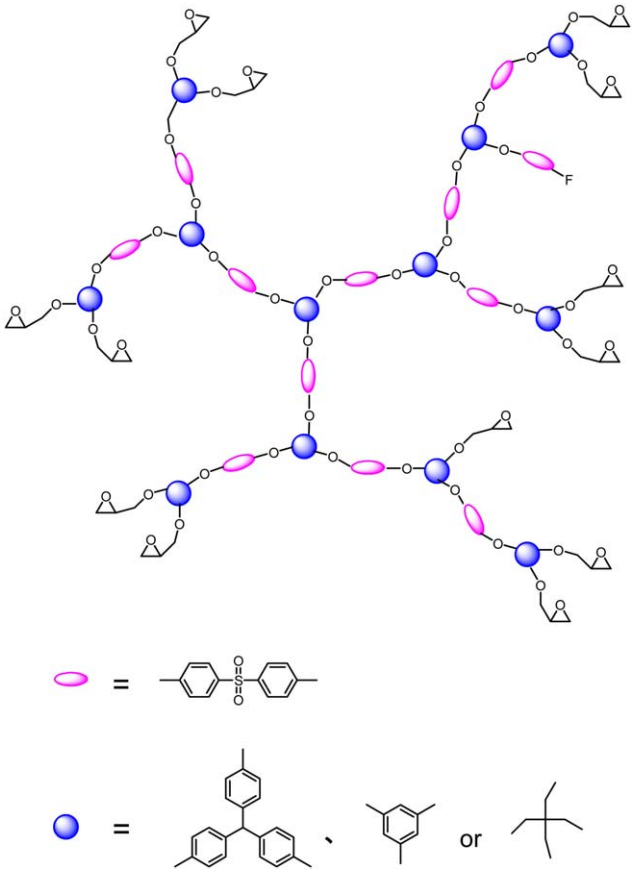

Figure 2. The ideal chemical structure of EHBPESs. [Color figure can be viewed in the online issue, which is available at wileyonlinelibrary.com.]

EHBPES should lead to higher ΔH_{tot}, which is beneficial for increasing crosslink density. However, at higher loadings (10% and 15%), ΔH_{tot} decreases with EHBPES3 loading, indicating that more incomplete cure occurs due to steric hindrance, which may lead to decreases in mechanical properties. For hybrids all contain 5% different EHBPES, the heats of reaction are shown in Table III. The hybrid containing 5% EHBPES3 has the highest ΔH_{tot}, which indicates that EHBPES3 has the highest extend of cure due to the smallest steric hindrance.

DMA Characterization

Effects of loading contents and backbone structure on storage moduli (E') and loss tangent (tanδ) are shown in Figure 4. For each composition, only one step change in E' and one corresponding peak are observed, suggesting no sign of phase separation, which is consistent with others studies.[18–20] As will be shown later, the cured hybrid containing EHBPES3, which has the most flexible backbone, shows the best overall performance. Thus, for simplicity, effects of loading are only demonstrated in the case of EHBPES3. As shown in Figure 4(a), the rubbery plateau modulus (E_r) increases with increasing EHBPES3 loading. Based on rubber rubbery elasticity,[35] the average crosslink density increases with EHBPES3 loading, which is expected due to the higher functionalities of EHBPES. As shown in Figure 4(b), below 10% loading, as EHBPES3 loading increases, T_g as defined by the peaks of tanδ also increases, which can be explained by higher crosslink density and more benzene rings in cured network, which is brought in by EHBPES. However, at 15% loading, T_g decreases slightly. The decrease in T_g could be related to more degree of incomplete cure in the terminal epoxide groups of EHBPES3 due to substitution effects at high loadings[36] (Table II). In addition, excessive loading of EHBPES3 also brings in lots of alkyl segments and leads to the dilution effects, which may override the effects of crosslink density and lead to a decrease in T_g.

Effects of backbone structure (at comparable degree of polymerization) on the temperature-dependent E' and tanδ are shown in Figure 4(c,d), respectively. It is clear that the hybrid containing EHBPES3 shows higher E_r and T_g than hybrids containing EHBPES1 and EHBPES2. The hybrid containing 5% EHBPES3 shows T_g of 156.6°C, which is 10.4°C higher than the neat system. Compared with EHBPES1 and EHBPES2, EHBPES3 has more flexible backbones, and the relatively flexible alkyl

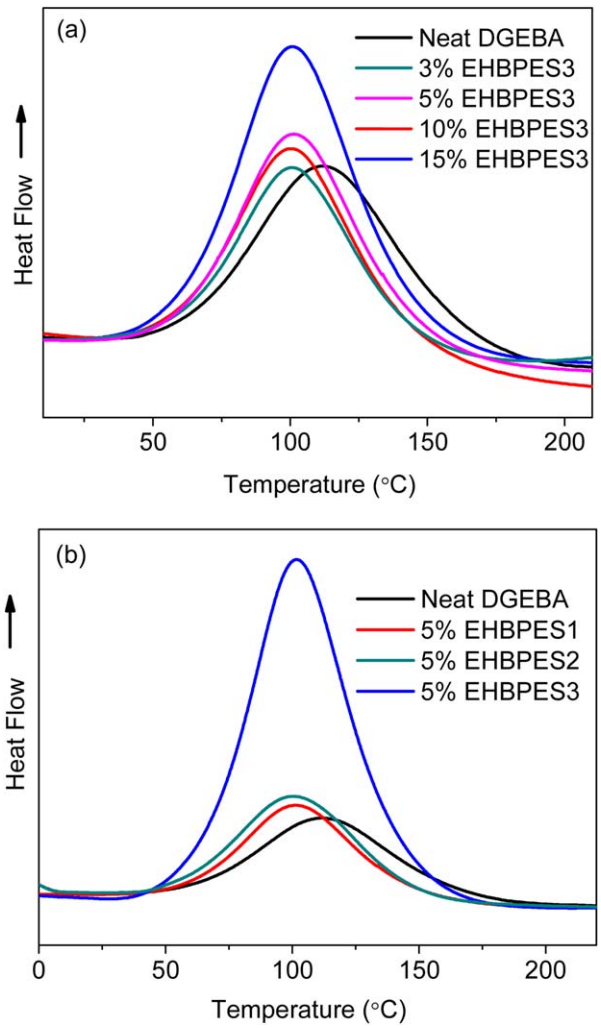

Figure 3. (a) DSC curves of cured neat DGEBA and hybrids with different EHBPES3 loadings. (b) DSC curves of cured neat DGEBA and hybrids with 5% EHBPES1, 5% EHBPES2, and 5% EHBPES3. [Color figure can be viewed in the online issue, which is available at wileyonlinelibrary.com.]

Table II. Thermal Properties of DGEBA/EHBPES3 Hybrids

Samples	$T_{g,DMA}$ (°C)	T_{d5} (°C)	ΔH_{tot} ($\times 10^{-4}$ J/mol)	Char yield at 800 °C (wt %)	Half-peak width of tanδ (°C)
Neat DGEBA	146.2	364.0	5.8	1.8	27.2
3% EHBPES3	155.6	365.1	7.3	5.3	16.3
5% EHBPES3	156.8	369.3	8.0	6.6	16.1
10% EHBPES3	161.2	370.2	7.6	8.8	15.8
15% EHBPES3	159.0	366.7	6.8	10.9	16.9

backbone of EHBPES3 can reduce steric hindrance and increase apparent average reactivity of terminal epoxy groups, which lead to higher crosslink density [Figure 3(b)].

In addition, the shape and the peak width of tanδ peaks could be related to miscibility and structural uniformity. As shown in Tables II and III, the half peak width (HPW) of hybrids is narrower than that of the neat system, suggesting that cured hybrids appear to be more uniform in structure than that of the neat system. At 3% and 5% loadings, values of HPW decrease, indicating that addition of EHBPES can lead to more uniform structure in cured hybrids, which is in agreement with other studies.[18–20] However, at 10% and 15% loadings, values of HPW increase. The increases in HPW at higher loadings can be explained by the incomplete cure (Table II). Although this finding is somewhat counterintuitive, it has also been confirmed in other's work.[18–20] Possible explanations could be that: (1) DMA is not sensitive enough to detect the nanoscale local inhomogeneous structures induced by addition of hyperbranched modifiers; (2) the added hyperbranched molecules can acted as core molecules in the early stage of cure and form more uniformed network structure at larger length scales, which is beyond the capability of DMA.

TMA Characterization of Cured Hybrids

Based on the classical free volume theory,[37] the fraction of free volume, f_T, can be expressed as:

$$f_T = f_g + \Delta\alpha(T - T_g),$$

where $\Delta\alpha = \alpha_r - \alpha_g$ is the difference between coefficients of thermal expansion (CTE) in the rubbery and glassy states, and f_g is the fractional free volume "frozen" at T_g. $\Delta\alpha$ could be treated as the CTE of free volume. This assertion has been confirmed by positron annihilation lifetime spectroscopy measurements.[19,20,37] As shown in Table IV, when EHBPES3 loading increases, α_g decreases and α_r increases. Thus, $\triangle\alpha$ which is related to the fractional free volume increases systematically with EHBPES3 loading, which is consistent with other studies.[18,38,39] The increases in fractional free volume with EHBPES3 loading can be explained by the inner cavity inside EHBPE3 and additional free volume between hyperbranched crosslinks. At the same 5% loading, α_g increases in the order of EHBPES1, EHBPES2, and EHBPES3, whereas α_r decreases in the order of EHBPES1, EHBPES2, and EHBPES3. Thus, $\triangle\alpha$ decreases in the order of EHBPES1, EHBPES2, and EHBPES3, which could be explained by the larger inner and additional free volume after addition of EHBPES3. In general, increasing fractional free volume leads to lower T_g. However, aside from fractional free volumes, T_g of cured network also depends on crosslink density and stiffness of the network chains. Addition of EHBPES increases both crosslink density and the density of aromatic structure in cured network, which can override higher fractional free volume and lead to an increase in T_g. The increase in fractional free volume could provide more room for possible kink motions[40] and thus improve the toughness of DGEBA/HBPEE hybrids, which will be discussed more in later sections.

Thermal Properties of Cured Hybrids

Effects of EHBPES3 loading on the thermal stability of cured hybrid are shown in Figure 5(a) and Table II. Below 10% loading, as EHBPES3 loading increases, the temperature which corresponds to 5% weight loss, T_{d5}, also increases, which is related to the network structure, including chemical composition, crosslink density, and perfection of network. Addition of multifunctional EHBPS3 increases the average crosslink (as shown in rubbery plateau moduli), which leads to higher T_{d5}. However, at 15% loading, T_{d5} decreases slightly, which is consistent with the trend in T_g. Similar to explanations offered to explained the T_g reduction at 15% loading, the decrease in T_{d5} can also be attributed to the dilution effects of alkyl segments and the unreacted terminal epoxide groups at excessive loading.[36]

Effects of backbone structure (at comparable degree of polymerization) on the thermal stability of the hybrids are compared in Figure 5(b) and Table III. The hybrid containing 5% EHBPES3

Table III. Thermal Properties of DGEBA/EHBPES Hybrids

Samples	$T_{g,DMA}$ (°C)	T_{d5} (°C)	ΔH_{tot} ($\times 10^{-4}$ J/mol)	Char yield at 800 °C (wt %)	Half-peak width of tanδ (°C)
Neat DGEBA	146.2	364.0	5.8	1.8	27.2
5% EHBPES1	150.2	342.0	5.7	4.0	19.6
5% EHBPES2	151.7	344.2	6.4	5.4	15.5
5% EHBPES3	156.8	369.3	8.0	6.6	16.1

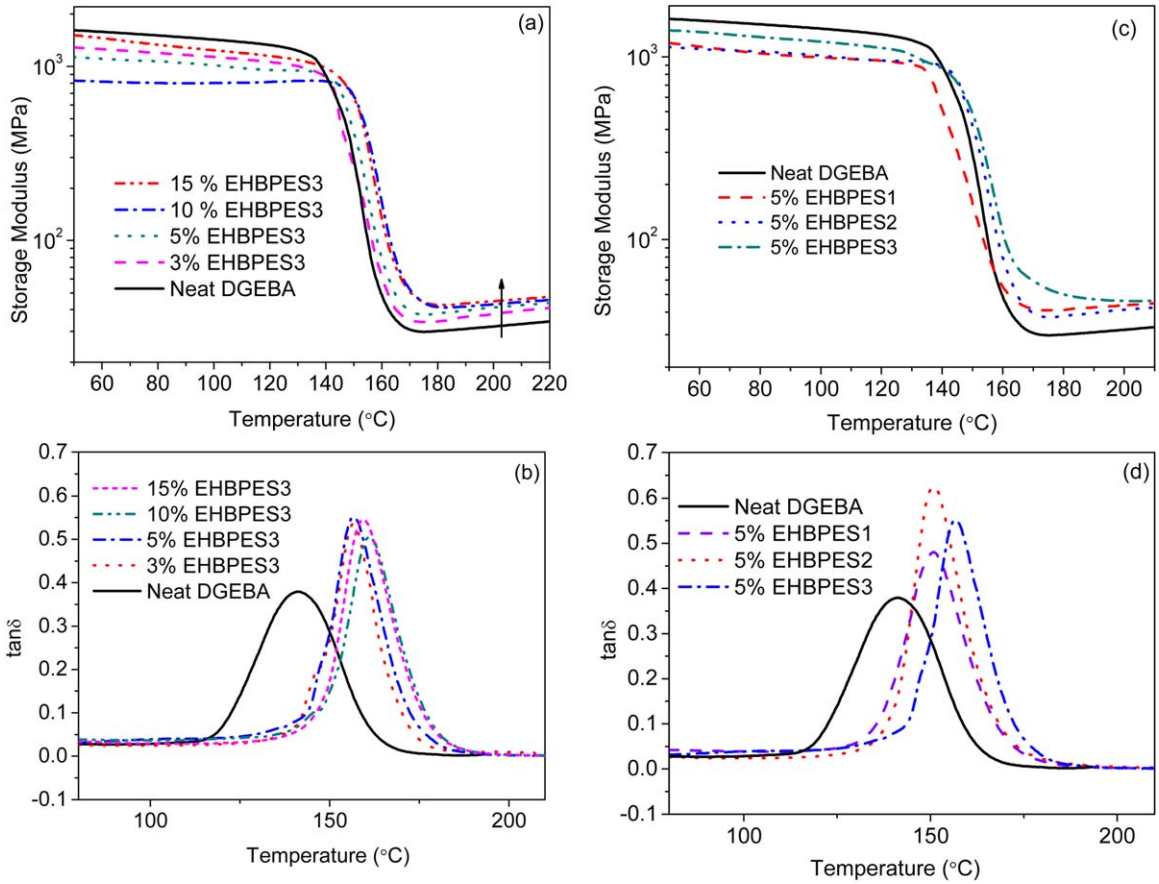

Figure 4. DMA results of DGEBA/EHBPESs hybrids. (a) Storage modulus and (b) tanδ of cured neat DGEBA and hybrids as a function of temperature with different EHBPES3 loadings; (c) storage modulus and (d) tanδ of cured neat DGEBA and hybrids s as a function of temperature with 5% EHBPES1, 5% EHBPES2, and 5% EHBPES3. [Color figure can be viewed in the online issue, which is available at wileyonlinelibrary.com.]

shows higher T_{d5} than those of EHBPES1 and EHBPES2. As already explained in the DMA section, at the same 5% loading, more flexible EHBPES3 can lead to more densely crosslinked network and better thermal stability.

Mechanical Properties

Effects of backbone structure on mechanical properties of cured hybrids are shown in Figure 6. Impact strength, tensile strength, and elongation at break all show similar general trends: those properties increase up to 5% loading and then decrease at higher loadings, which is consistent with other studies.[22,28,35,37,39] In addition, we note that the optimum impact properties are always achieved at ~5% EHBPES loading irrespective of backbone structure. It is known to us that HBPs have much more end groups than DGEBA molecules. Thus, the terminal epoxide groups on HBPs tend to have higher reactivity and can be more easily incorporated into the network during the early stage of cure,[41] which leads to acceleration of gelation.[42] As a result, the hyperbranched molecule can build up a percolation scaffold in the early stage of cure. Each percolation scaffold build by hyperbranched molecule and its connecting regions can be treated as "effective sphere".[43] Just as Liu *et al.*[40] proposed that once those effective spheres percolate through the inhomogeneous epoxy network, toughness and other performance are greatly improved. Thus, the size of EHBPES may not be a defining factor. In addition, it is well known that the atomic packing factor (APF) in metal is independent of the size of monodispersed hard spheres.[44] Although, the size of the EHBPES molecules is not uniform and strictly spherical, this analogy may still be useful in explaining when optimum performance always occurs at about 5% loading and shows weak backbone structure dependence.

Table IV. Linear Coefficients of Thermal Expansion of Hybrids

Sample	α_g ($\times 10^{-6} \times K^{-1}$)	α_r ($\times 10^{-6} \times K^{-1}$)	$\triangle\alpha = \alpha_r - \alpha_g$ ($\times 10^{-6} \times K^{-1}$)
Neat DGEBA	92.5	188.1	95.6
3% EHBPES3	91.9	189.9	98.0
5% EHBPES3	90.2	192.7	102.5
10% EHBPES3	88.4	193.5	105.1
15% EHBPES3	83.1	195.3	112.2
5% EHBPES1	84.6	194.1	109.5
5% EHBPES2	87.3	193.0	105.7

When the loading is $\leq$5%, elongation at break, impact strength, and tensile strength all increase with EHBPES loading. As discussed in DMA and TMA sections, increasing EHBPES loading

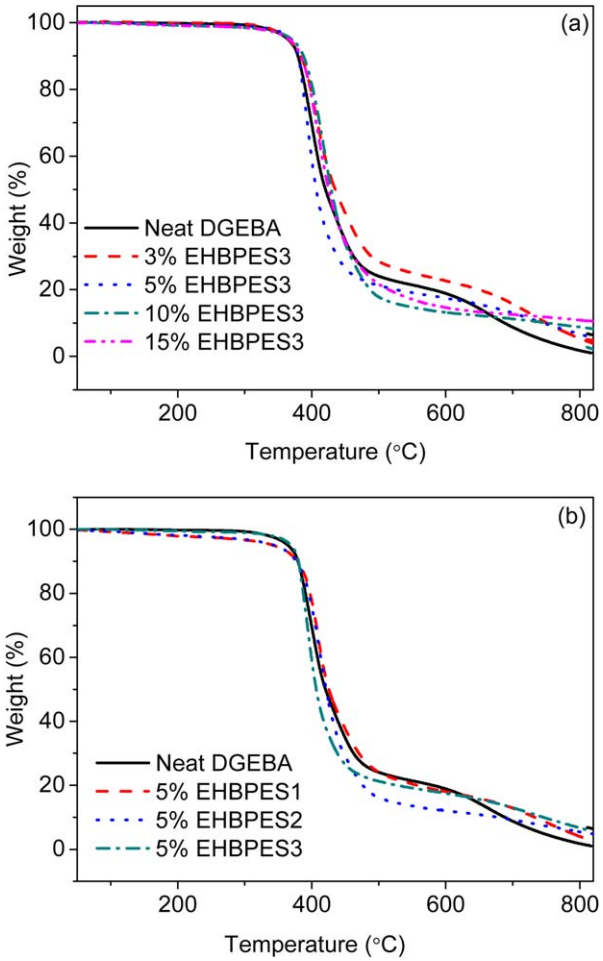

Figure 5. (a) TGA curves of cured neat DGEBA and hybrids with different EHBPES3 loadings. (b) TGA curves of cured neat DGEBA and hybrids with 5% EHBPES1, 5% EHBPES2, and 5% EHBPES3. [Color figure can be viewed in the online issue, which is available at wileyonlinelibrary.com.]

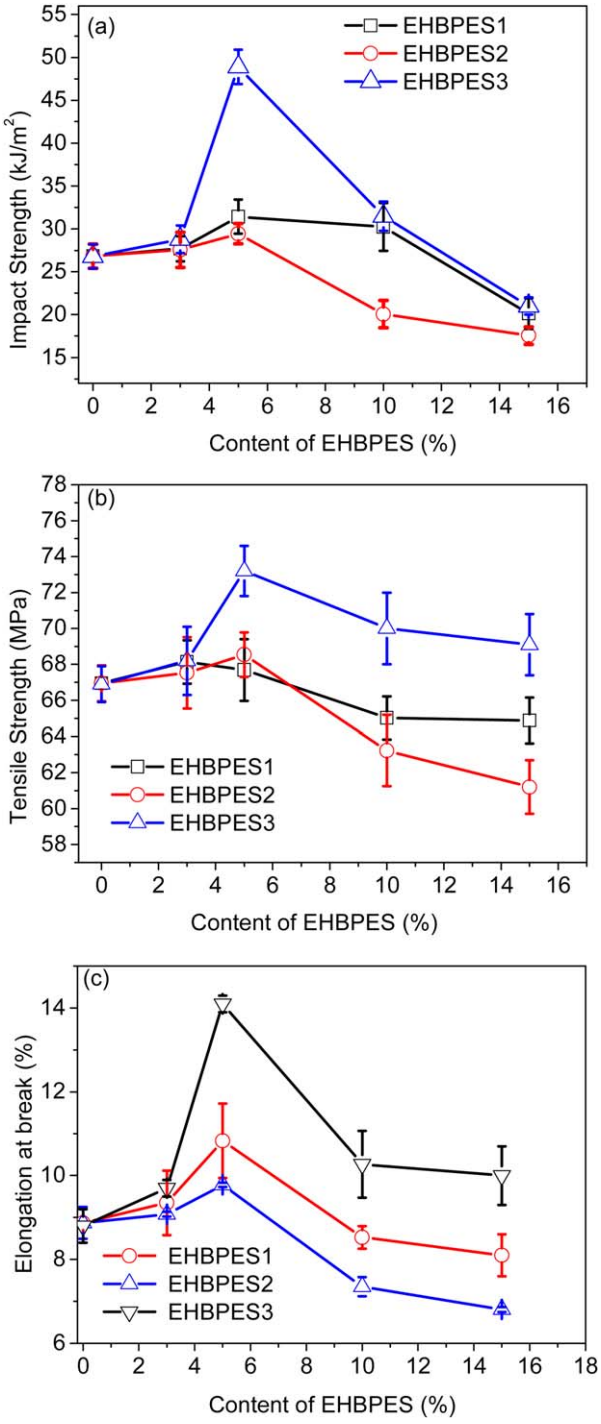

Figure 6. Effects of EHBPES content on (a) impact strength, (b) tensile strength, and (c) elongation at break. [Color figure can be viewed in the online issue, which is available at wileyonlinelibrary.com.]

leads to simultaneous increases in average crosslink density and fractional free volume. The increase in fractional free volume can be used to explain the increases in impact strength and elongation at break; whereas, higher crosslink density is beneficial for tensile strength. However, mechanical properties decrease at high EHBPES loadings (10% and 15%). As already shown in sections of DMA and thermal properties, more terminal groups are left unreacted at high loadings due to steric hindrance. Those unreacted dangling chain ends can act as defects and lower mechanical properties. Clearly, the hybrid containing 5% EHBPES3, which has the most flexible backbone structure, shows the best overall performance. Compared with neat system, it shows 69.8% increase in impact strength (i.e., 48.9 kJ/m^2), 9.4% increase in tensile strength (i.e., 73.2 MPa), and a 60.2% increase in elongation at break (i.e., 14.1%). At 5% loading, all three EHBPESs can simultaneous improve toughness, strength, elongation at break, and the glass transition temperature; however, EHBPES3 is the most effective. As mentioned in the introduction, enhancing the impact strength without compromising tensile strength and T_g still remains a big challenge, especially for nonphase separated tougheners. The remarkable balanced improvements in toughness, tensile strength, and elongation at break as well as T_g show that EHBPES3 is a very powerful all-purpose modifier for epoxy, and possible explanations are offered below. First, the backbone of EHBPES3 contains both aromatic and aliphatic moieties, which combines some degrees of stiffness and flexibility in one molecule. This

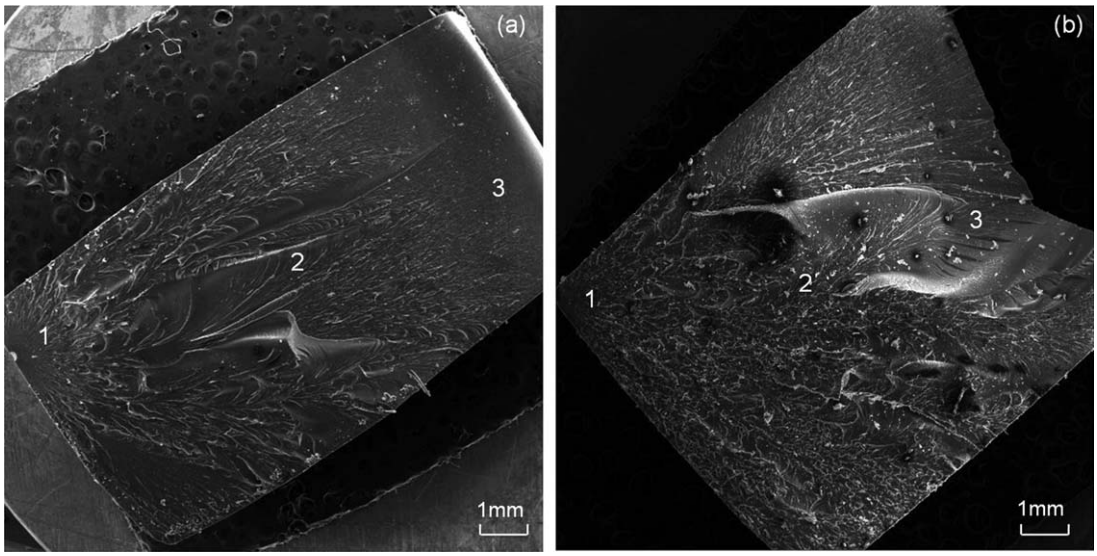

Figure 7. SEM images of the fracture surface of (a) neat epoxy and (b) DGEBA/EHBPES3 hybrid with 5% loading in macroscopic state.

unique combination imparts balanced improvements in tensile strength and toughness, in some sense similar to the bimodal distribution rubber. The flexible alkyl carbon segments in EHBPES3 can reduce the steric hindrance and lead to more densely crosslinked network, which is beneficial to the increases in T_g, thermal stability and strength. In the meantime, the aromatic rings in EHBPES can override the dilution effects and lead to a increase in T_g. Second, in spite of steric hindrance effects, the higher functionality of EHBPES can increase the average crosslink density of the network, which increases T_g, thermal stability, and strength. Third, although the average crosslink density is increased, the fractional free volume also

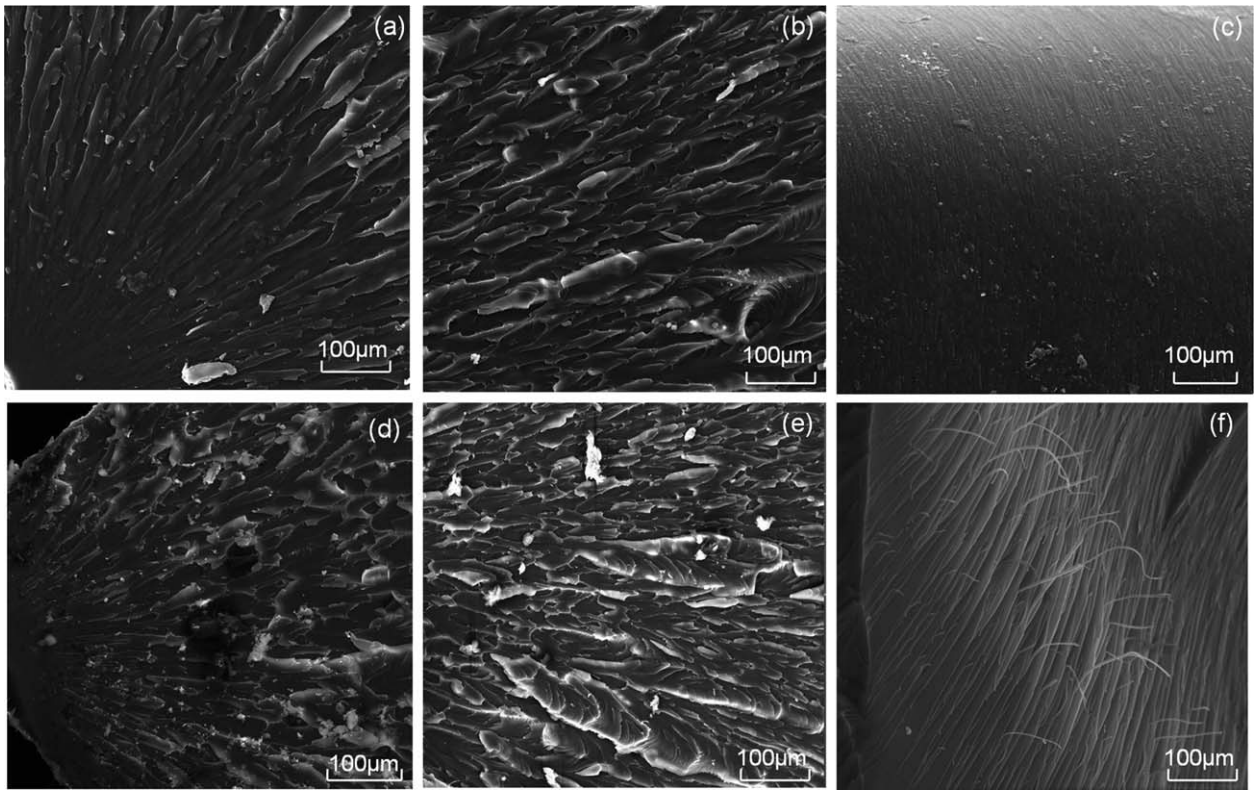

Figure 8. SEM micrographs of the impact fracture surface in different positions but same magnification time: neat DGEBA (a) the initial crack point of fracture surface, (b) the middle area of fracture surface, (c) the rear area of fracture surface; DGEBA/EHBPES3 hybrid (d) the initial crack point of fracture surface, (e) the middle area of fracture surface, and (f) the rear area of fracture surface.

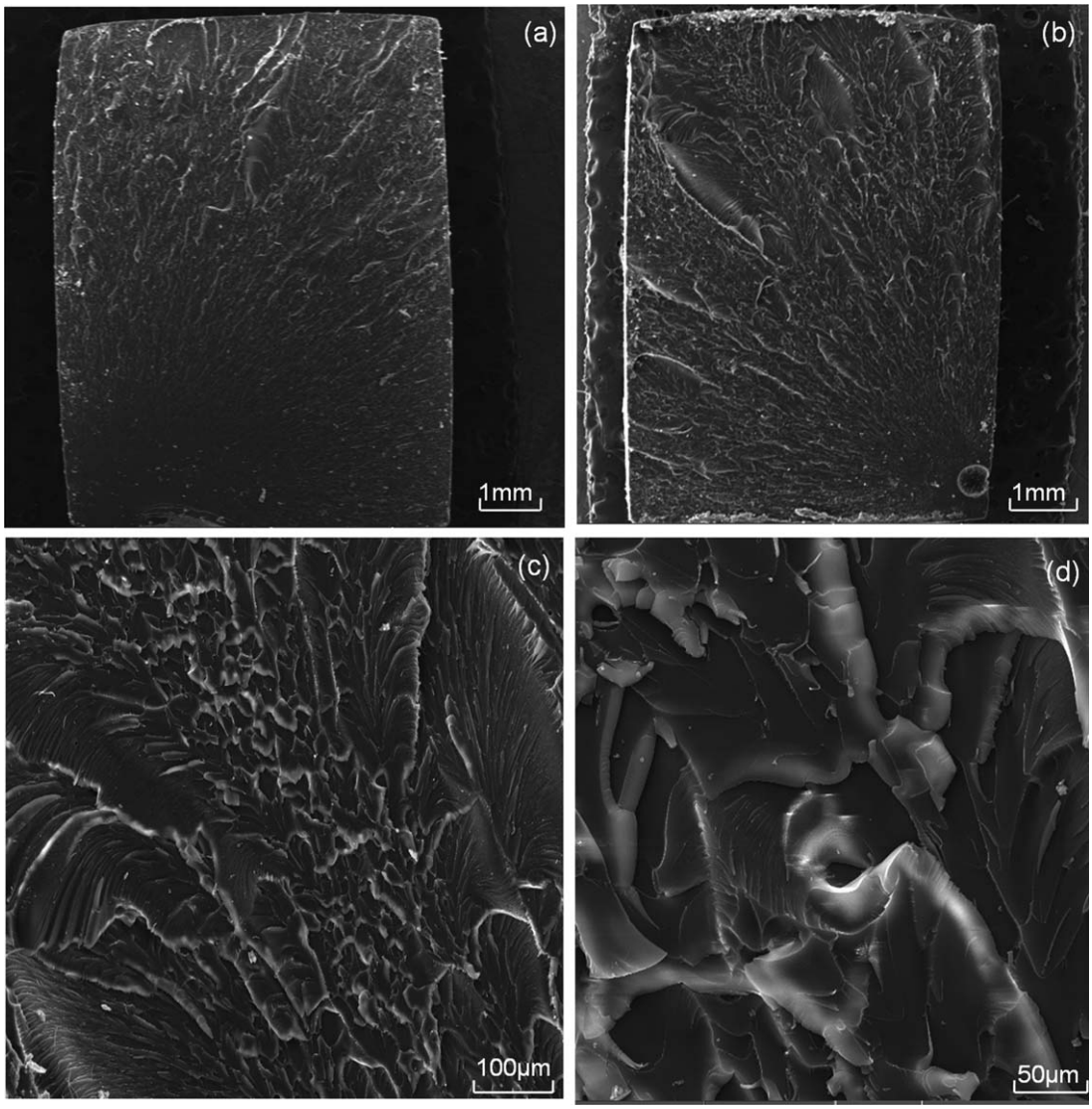

Figure 9. SEM images of tensile fracture surface: (a) neat epoxy and (b) DGEBA/EHBPES3 hybrid with 5% loading in macroscopic state; (c) the rear area of fracture surface of DGEBA/EHBPES3 hybrid with 5% loading; and (d) enlarged view of image of the rear area of fracture surface of DGEBA/EHBPES3 hybrid with 5% loading.

increases, which may deform under impacts and improve toughness.[22,28,29] Forth, the semispherical hyperbranched molecules can form crosslinked arms in different radial directions. Thus, under tension or impacts, the local stress could be readily redistributed to different directions through its many network strands and lead to a more effective load transfer, which may help to improve both strength and toughness.[40]

Morphology Analysis

After impact tests, fracture surfaces of cured neat system and the hybrid with 5% EHBPES3 are shown in Figure 7(a,b), respectively. No cavities are observed indicating no sign of phase separation, which is consistent with DMA measurements. Clearly, the fracture surface of hybrid [Figure 7(b)] is much rougher than that of the neat system [Figure 7(a)]. Obvious "humped" structures in radial directions and stress-whitened zones are observed in cured hybrids. Enlarged views at different positions of fracture surfaces in both systems are shown in Figure 8. Figure 8(a–c) correspond positions 1, 2, and 3 of Figure 7(a), respectively. Figure 8(d–f) correspond to positions 1, 2, and 3 of Figure 7(b), respectively. The breaking process of hybrids is more clearly shown in Figure 8(d–f). Starting from the crack initiation point [Figure 8(d,e)], the size of yield increases with distance, shows stress whitening [Figure 8(d)], and then show fibrils at the end [Figure 8(f)]. Both shear yielding, which is often evident as stress whitening zones, and fibrils are important energy dissipating mechanisms,[21,45] which lead to higher impact strength and higher elongation at break.

Compared with impact tests, the tensile test is a slow deformation process and may reveal additional information on deformation process. Fracture surfaces after tensile tests for neat system and hybrid containing 5% EHBPES3 are shown in Figure 9(a,b), respectively. Clearly, the fracture surface of hybrid is also

rougher than that of the neat system. Enlarged views at the rear side (i.e., far away from the break initiation point) of the hybrid at 5% EHBPES3 loading is shown in Figure 9(c). For hybrid samples, the general feature of fracture surface after tensile test is similar to that after impact test, suggesting that the main toughening mechanisms are operative in both cases. However, no obvious fibrils were found on the fracture surface after tensile test; instead, some "dimple-like" structure is more clearly seen in the fracture surface after tensile test [Figure 9(d)]. In impact tests, when the crack propagating speed reaches its limits, fibrils are often formed. In contrast, when subjected to low speed tensile test, the network strands in hybrids have more time to respond to external forces and form dimples rather than fibrils.

CONCLUSIONS

Epoxide-terminated hyperbranched polyether sulphones with different backbone structures were synthesized and used as tougheners for DGEAB/TETA curing system. Effects of backbone structure and loading amounts on the mechanical and thermal performances were investigated. DMA and SEM results reveal no sign of phase separation in all hybrids. Interesting, optimum mechanical performance is always achieved at 5% loading despite the different backbone structure, which may related to the percolation of "effective spheres", and the hybrid containing 5% EHBPES3, which has the most flexible backbone, shows the best balanced improvements in impact strength, tensile strength, elongation at break, and T_g, showing an increase of 69.8%, 9.4%, 60.2%, and 7.1%, respectively, as compared to the unmodified system. Thus, EHBPES3 can be used as an all-purpose modifier for epoxy without forming phase-separated morphology. The balanced improvements can be ascribed to the unique structure (i.e., nanoscale inhomogeneous network with higher crosslink density and higher fractional free volume), which depends on the structure and the loading amounts of hyperbranched modifiers. The flexibility of constituting units in EHBPES appears to play an important role. The more flexibility EHBPES3 ensures that more terminal epoxide groups can be reacted, which leads to more densely crosslinked network and less network defects. Both rigid and flexible units are combined properly in the backbone of EHBPES3. Thus when added in proper amount, it can increase both crosslink density and the fractional free volume without introduce too much dilution effects. In addition, the hyperbranched crosslinking points can more effectively redistribute external loads in all radial arms and lead to further improvements in toughness.

ACKNOWLEDGMENTS

This work is financially supported by the National Natural Science Foundation of China (Grant number 51173012).

REFERENCES

1. Lee, H.; Neville, K. Handbook of Epoxy Resins; McGraw-Hill: New York, **1967**.
2. Bouer, R. S. Epoxy Resin Chemistry; American Chemical Society: Washington, DC, **1983**.
3. LeMay, J.; Kelley, F. Advances in Polymer Science; Springer: Berlin/Heidelberg, **1986**; pp 115−148.
4. Liang, Y. L.; Pearson, R. A. *Polymer* **2010**, *51*, 4880.
5. Gan, W.; Zhan, G.; Wang, M.; Yu, Y.; Xu, Y.; Li, S. *Colloid. Polym. Sci.* **2007**, *285*, 1727.
6. Pillai, J. P.; Pionteck, J.; Häßbler, R.; Sinturel, C.; Mathew, V. S.; Thomas, S. *Ind. Eng. Chem. Res.* **2011**, 51, 2586.
7. Nguyen, F. N.; Berg, J. C. *Compos. Part A* **2008**, *39*, 1007.
8. Wu, S. *Polymer* **1985**, *26*, 1855.
9. Pearson, R. A.; Yee, A. F. *Polymer* **1993**, *34*, 3658.
10. Hedrick, J. L.; Yilgor, I.; Jurek, M.; Hedrick, J. C.; Wilkes, G. L.; McGrath, J. E. *Polymer* **1991**, *32*, 2020.
11. Wilkinson, S. P.; Ward, T. C.; McGrath, J. E. *Polymer* **1993**, *34*, 870.
12. Kunz, S. C.; Sayre, J. A.; Assink, R. A. *Polymer* **1982**, *23*, 1897.
13. Gao, C.; Yan, D. *Prog. Polym. Sci.* **2004**, *29*, 183.
14. Mezzenga, R.; Boogh, L.; Månson, J. A. E. *Compos. Sci. Technol.* **2001**, *61*, 787.
15. Morell, M.; Ramis, X.; Ferrando, F.; Yu, Y.; Serra, A. *Polymer* **2009**, *50*, 5374.
16. Zhang, D.; Liang, E.; Li, T.; Chen, S.; Zhang, J.; Cheng, X.; Zhou, J.; Zhang, A. *RSC Adv.* **2013**, *3*, 3095.
17. Zhang, D.; Liang, E.; Li, T.; Chen, S.; Zhang, J.; Cheng, X.; Zhou, J.; Zhang, A. *RSC Adv.* **2013**, *3*, 9522.
18. Luo, L.; Meng, Y.; Qiu, T.; Li, X. *J. Appl. Polym. Sci.* **2013**, *130*, 1064.
19. Lv, J.; Meng, Y.; He, L.; Qiu, T.; Li, X.; Wang, H. *J. Appl. Polym. Sci.* **2013**, *128*, 907.
20. Luo, L.; Meng, Y.; Qiu, T.; Li, Z.; Yang, J.; Cao, X.; Li, X. *Polym. Compos.* **2013**, *34*, 1051.
21. Ratna, D.; Simon, G. P. *J. Appl. Polym. Sci.* **2010**, *117*, 557.
22. Zhang, D.; Chen, Y.; Jia, D. *Polym. Compos.* **2009**, *30*, 918.
23. Yan, D.; Gao, C.; Frey, H. Hyperbranched Polymers: Synthesis, Properties, and Applications; Wiley: Hoboken, **2011**; pp 1−22.
24. Voit, B. I.; Lederer, A. *Chem. Rev.* **2009**, *109*, 5924.
25. Ratna, D.; Varley, R.; Simon, G. P. *J. Appl. Polym. Sci.* **2003**, *89*, 2339.
26. Ratna, D.; Varley, R.; Raman, R. K. S.; Simon, G. P. *J. Mater. Sci.* **2003**, *38*, 147.
27. Foix, D.; Serra, A.; Amparore, L.; Sangermano, M. *Polymer* **2012**, *53*, 3084.
28. Zhang, D.; Jia, D. J. *Appl. Polym. Sci.* **2006**, *101*, 2504.
29. Chen, S.; Zhang, D.; Jiang, S.; Jia, D. *J. Appl. Polym. Sci.* **2012**, *123*, 3261.
30. Jin, F. L.; Park, S. J. J. *Polym. Sci. Part B: Polym. Phys.* **2006**, *44*, 3348.
31. Gong, C.; Fréchet, J. M. *J. Macromolecules* **2000**, *33*, 4997.
32. Hawker, C. J.; Malmström, E. E.; Frank, C. W.; Kampf, J. P. J. J. *Am. Chem. Soc.* **1997**, *119*, 9903.
33. Roy, R. K.; Ramakrishnan, S. *Macromolecules* **2011**, *44*, 8398.

34. Hawker, C. J.; Lee, R.; Fréchet, J. M. J. *J. Am. Chem. Soc.* **1991**, *113*, 4583.
35. Ngai, K. L.; Roland, C. M. *Macromolecules* **1993**, *26*, 2688.
36. Mezzenga, R.; Boogh, L.; Månson, J. A. E. *Macromolecules* **2000**, *33*, 4373.
37. Strobl, G. The Physics of Polymers: Concepts for Understanding Their Structures and Behavior; Springer-Verlag: Berlin, **2007**, pp 245−286.
38. Arasa, M.; Ramis, X.; Salla, J. M.; Ferrando, F.; Serra, A.; Mantecón, A. *Eur. Polym. J.* **2009**, *45*, 1282.
39. Liu, W.; Zhou, R.; Goh, H. L. S.; Huang, S.; Lu, X. *Appl. Mater. Interfaces.* **2014**, *6*, 5810.
40. Liu, T.; Nie, Y.; Chen, R.; Zhang, L.; Meng, Y.; Li, X. *J. Mater. Chem. A* **2015**, *3*, 1188.
41. Flory, P. J. Principles of Polymer Chemistry; Cornell University Press: New York, **1953**, Chapter 4.
42. Li, Q.; Li, X.; Meng, Y. *Thermochim. Acta* **2012**, *549*, 69.
43. Riew, C. W.; Kinloch, A. J. Toughened Plastics II: Novel Approaches in Science and Engineering; American Chemical Society: Washington, D.C., **1996**, Chapter 17, pp 251−277.
44. Callister, W. D. Jr. Materials Science and Engineering: An Introduction, 6th ed. Replika Press: India, **2003**, Chapter 3, pp 31−38.
45. Ratna, D.; Varley, R.; Raman, R. K. S.; Simon, G. P. *J. Mater. Sci.* **2003**, *38*, 147.